UDC 620 . 186 . 5 : 539 . 4 . 072

Technical Report

Phase-field Simulation of Grain Growth

Yoshihiro SUWA*

Abstract

Grain growth occurring in the steel manufacturing process is one of the most important phenomena in order to control the polycrystalline microstructure. Due to its heavy computational cost, phase-field(PF) simulations were limited to 2D systems. Recently, 3D PF simulation of grain growth is becoming practical owing to the development of efficient simulation algorithms and the application of parallel computation techniques. In this manuscript, we will report simulation results for the normal grain growth and the system containing finely dispersed second-phase particles. Especially, this manuscript highlights the difference between the 2D and 3D simulation results.

1. Introduction

The crystal structure of a polycrystalline material is a key factor in determining the physical properties of the material. Also, the growth of grains that occurs in the steel manufacturing process is one of the most important metallurgical phenomena from the standpoint of controlling the crystal structure of steel. It is, however, difficult to incorporate the geometric characteristics of crystal structures directly in an analytical theory on grain growth.[1-5] In this respect, the numerical analysis of grain growth by computer simulations is generally considered promising, and various simulation models, including the Monte Carlo (MC) method, have been proposed.[6-19]

In recent years, attempts have been actively made to apply the phase-field (PF) method, which has progressed remarkably in the field of computational material science, to grain growth simulations.[14-19] The most important advantage of using the PF method for modeling is that since the crystal interfaces are naturally introduced into the model as parts whose order parameter gradient is not zero, it is unnecessary to trace the interfaces themselves. In addition, by taking into account the anisotropy of interfacial energy and mobility, it is possible to make a more realistic analysis of grain growth. Furthermore, by adding concentration field as an extra order parameter, it is possible to naturally introduce the long-range diffusion that is required when modeling the segregation of a solute element,[20] or the coarsening of a dispersed secondary phase.[21]

Despite the above advantages, the application of the PF method in grain growth simulations had been almost limited to 2-D simulations because of the heavy computational cost. However, with the improvement in simulation algorithms,[22-24] coupled with the application of parallel computation techniques in recent years,[25-27] there are more and more reports on the application of the PF method in three-dimensional simulations. This paper describes the results of the grain growth simulations that the author has so far carried out using the PF method,[26, 27] with the emphasis on the difference between 2-D and 3-D simulation results.

2. Model

2.1 Phase-field polycrystalline grain growth model

The PF method is a simulation model based on non-equilibrium thermodynamics. It first attracted attention as it permitted reproduction of the complicated structural formation of dendrite. Today, the scope of its application has been expanded to diffusion phase decompositions (nucleation, spinodal decomposition, Ostwald ripening, etc.), order-disorder transformation, various types of domain growth (dielectric substance, magnetic substance), martensitic transformation/shape memory, and solid phase crystal growth/recrystallization, etc. Thus, the PF method is becoming a very effective simulation method for prediction and analysis of microstructural forma-

* Senior Researcher, Dr.Eng., Sheet Products Lab., Steel Research Laboratories
20-1, Shintomi, Futtsu, Chiba 293-8511

tion at both the nano and meso scales.[28, 29)]

The polycrystalline grain growth model applying the PF method is a model for predicting the behavior of grain growth on the assumption that the interface moving velocity is proportional to the local mean curvature.[30)] Ordinarily, the model expresses grain orientation using many order parameters (multiple orientation-fields model: MOFM)[14-18)] or only one order parameter (for 2-D simulations) (single orientation-field model: SOFM).[14-19)] In terms of the computational cost involved, SOFM is advantageous. However, taking into consideration the expandability to a 3-D system, the ease of introduction on interfacial energy/mobility anisotropy, and the coupling with other order parameters such as concentration field of solute, MOFM is more practical at present. All the simulation results described in this paper were obtained using MOFM. As a representative example of MOFM, the multi-phase-field (MPF) model developed by Steinbach et al.[31)] is outlined below.

In the MPF method, a set of continuous order parameters ϕ_i (i = 1, 2, ..., N) is defined as distinguishing between virtual grain orientations, with N denoting the total number of order parameters. The value of $\phi_i(\vec{r}, t)$ indicates the probability of the existence of a grain having grain number i at position $\vec{r}$ and time t. Within the grain labeled ϕ_1, the absolute value for ϕ_1 is 1, while all other ϕ_i for $i \neq 1$ is zero. The term "virtual grain orientation" was used above because it does not indicate the actual grain orientation: it is used simply to distinguish between different regions. It should be noted, however, that it is possible to associate virtual orientations with actual grain orientations and thereby perform an analysis taking the actual orientations into consideration.[32)]

In this model, the sum of phase fields at any position in the system is conserved.

$$\sum_{i=1}^{N} \phi_i(\vec{r}, t) = 1 \qquad (1)$$

Here, we outline the equations from the MPF model, which are essential for this study. The model details are described in Reference 33). When considering the grain growth only, the set of governing equations to be solved is as follows.

$$\frac{\partial \phi_i}{\partial t} = -\frac{2}{n(\vec{r}, t)} \sum_{j \neq i}^{N} s_{ij} M_{ij} \left[\frac{\delta F}{\delta \phi_i} - \frac{\delta F}{\delta \phi_j} \right], \quad (i = 1 \cdots n) \qquad (2)$$

Where F is the free energy functional of the system and M_{ij} is the mobility of interface in the PF method. From the above equation, the following equation can be derived.

$$\frac{\delta F}{\delta \phi_i} = \sum_{j \neq i}^{N} \left[\frac{\varepsilon_{ij}^2}{2} \nabla^2 \phi_j + \omega_{ij} \phi_j \right] + f_i^E \qquad (3)$$

Where ε_{ij} is the energy gradient coefficient, ω_{ij} is the double-well potential depth, and f_i^E is the excess free energy density of grain having grain number i. By adjusting ε_{ij} and ω_{ij} simultaneously, it is possible to control the interfacial energy.[33)] In addition,

$$n(\vec{r}, t) = \sum_{i=1}^{N} s_i(\vec{r}, t). \qquad (4)$$

Where $s_i(\vec{r}, t)$ is a step function that satisfies $s_i(\vec{r}, t) = 1$ when $\phi_i > 0$ and $s_i(\vec{r}, t) = 0$ otherwise.

By obtaining the numerical solution to Equation (2) using methods such as the differential method, it is possible to predict the behavior of grain growth.

2.2 Improving simulation efficiency

As a problem involved in the MOFM polycrystalline grain growth model, the coalescence of grains with the same grain number is cited. This is a problem common with the MC method and MOFM. In 2-D simulations, in order to prevent the total number of orientations, N, from influencing the rate of grain growth, it is necessary that N be 100 or more.[22)] With the MC method, for example, the efficiency of simulation decreases as N is increased. This problem can be solved by improving the algorithm of state transition. With MOFM, however, the memory capacity required increases in proportion to N and the computing time increases in proportion to the square of N in the worst case. This means that using an extremely large value of N is impracticable. Therefore, it is necessary to work out a method of preventing the coalescence of grains without significantly increasing the value of N.

Taking advantage of the fact that the free energy of a system remains the same even when the orientation is switched between equivalent crystal orientations during simulation, Krill et al.[22)] improved the efficiency of simulation by reducing the value of N required. Suwa et al. extended the above improvement in simulation efficiency to a system which takes into consideration the anisotropy of the interface,[25)] and a system which contains dispersed particles.[26)] After that, more sophisticated algorithms were devised by Vedantam et al.[23)], Gruber et al.,[24)] and Kim et al.[18)] Their algorithms have eliminated the problem of "coalescence." It is interesting to note that the above refined algorithms, which are the same in principle, were developed by three different study groups around the world at almost the same time.

3. Simulation Results

3.1 Simulation of normal grain growth of single-phase material

This section describes the results of our simulation of a single-phase material in which the same interfacial energy and mobility were given to all the interfaces.[27)] Those conditions represent the most simplified, and most important, system in studying the behavior of polycrystalline grain growth. Whenever a new simulation model is developed, therefore, this system is used as the primary benchmark.

Fig. 1 shows the simulated time evolution of the microstructure. The number of grains, N_g, is 35,174 at t = 500 Δt and 1,185 at t = 10,000 Δt. With the PF method, by setting the parameters properly, it is possible to carry out a numerical simulation taking into account the actual time and the actual space size. In this report, however, with preference given to simplicity, the time is expressed by time differential interval Δt and the space size is expressed by space differential interval Δx. **Fig. 2** shows the time evolution of the square of average grain radius <R>. The obtained result can be approximated by a straight line and the rate of grain growth meets the well-known one-half power law.

In the case of normal grain growth, it has been known that the "steady state,"[3)] in which the size distribution function normalized by average grain diameter is time invariant, is reached after a certain simulation time. For the purpose of comparing the size distribution function in the steady state, **Fig. 3** shows the result of our simulation, the result of a simulation performed by Kim et al. using a similar model,[18)] and the result of an mean field analysis by Hillert et al.[3)] It can be seen from the figure that the grain size distribution we obtained is somewhat wider and more symmetrical than that of Kim et al. This slight difference in grain size distribution is considered due to an imperfect steady state in the simulation performed by Kim et al.[27)]

Recently, 3-D microstructural observations are also being made possible. However, microstructural photos obtained by ordinary ex-

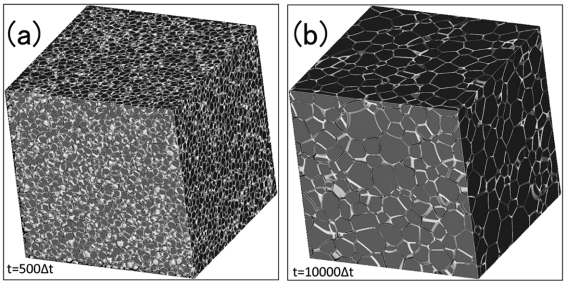

Fig. 1 Simulated microstructural evolution in 512^3 cells (a) 35,174 grains at t = 650 Δt and (b) 1,185 grains at t = 10,000 Δt

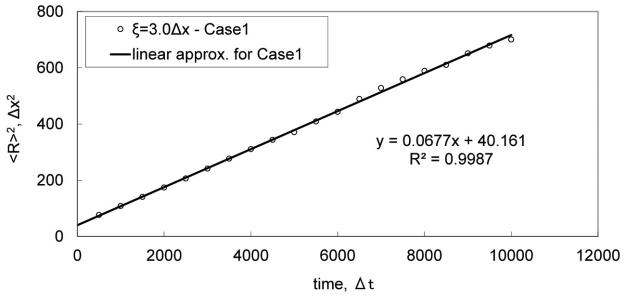

Fig. 2 Square of average grain radius $\langle R\rangle^2$, versus simulation time The thick straight line is the linear least-square fitting for a simulation run.

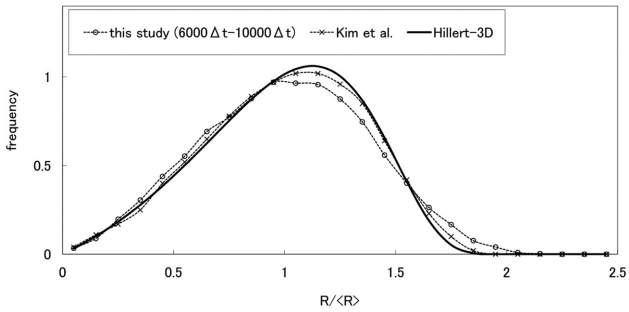

Fig. 3 Steady-state grain size distributions from various phase-field simulations of the 3D normal grain growth Kim et al.[18] (MPF model, symbols were taken from Fig.15 in Ref. 18) and our study (MPF model + APT algorithm). The thick curve depicts the 3D distribution predicted by Hillert theory[3].

perimental observations show 2-D sections of 3-D structures. For the purpose of comparing a 3-D structure and its 2-D section, **Fig. 4** shows the grain size distribution reconstructed from the set of 2-D slices of a 3-D structure obtained by our simulation. A comparison between Fig. 3 and Fig. 4 reveals that the grain size distribution shifts toward the small size for the 2-D slices. Assuming the average grain radius obtained from 2-D slices as $\langle R_{2d}\rangle$, $\langle R\rangle \approx 1.18 \langle R_{2d}\rangle$. It should be noted here that the steady-state grain size distribution obtained in 2-D simulation is different from the one reconstructed from a 3-D structure or its 2-D section.[3, 18]

Next, we consider the behavior of individual grain growth. In the

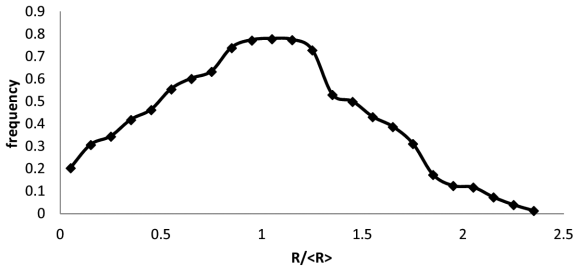

Fig. 4 Steady-state grain size distributions reconstructed from a set of 2D slice of 3D microstructure

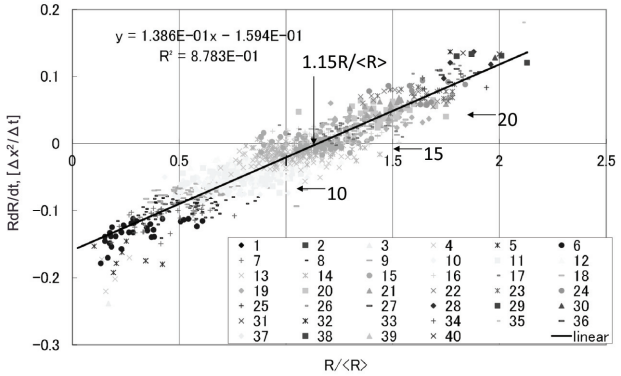

Fig. 5 Simulation test of mean-field approximation [Eq.(5)] in the 3D normal grain growth The results obtained from a simulation run at t = 10,000 Δt is shown in this figure, where 1,185 grains are shown as dots in a RdR/dt vs R/<R> plane. The dR/dt values were measured from the volume changes during a single time step. The thick straight line is the linear least-square fitting.

mean field analysis by Hillert, the growth rate of individual grains is expressed by the following equation.[3]

$$\frac{dR}{dt} = \alpha M_p \sigma \left(\frac{1}{R_c} - \frac{1}{R}\right) : \; R\frac{dR}{dt} = \alpha M_p \sigma \left(\frac{R}{R_c} - 1\right) \qquad (5)$$

Where R is the radius of the grain under consideration and R_c is the critical grain radius. From the above equation, grains larger than R_c grow, whereas grains smaller than R_c shrink. In addition, M_p denotes physical interface mobility, σ is the interfacial energy, and α the correction value (≈ 1) for taking into consideration the detailed geometric influence not included in the mean field approximation. In order to evaluate the above equation, Kim et al. carried out an analysis using the relationship between RdR/dt and $R/\langle R\rangle$.[18]

By following Kim's treatment, we show the relationship between RdR/dt and $R/\langle R\rangle$ for individual grains at t = 10,000 Δt in **Fig. 5**. From the figure, the value on the x-axis at the point of intersection with the approximate straight line, or the critical grain radius, is 1.15. This result closely reproduces the result obtained by Kim et al. and agrees very well with the result of Hillert's mean field analysis, $R_c = 9/8 \langle R\rangle = 1.125 \langle R\rangle$. Therefore, in the 3-D crystal grain growth, it is possible to judge the expansion or shrinkage of each individual grain using the radius, R, of the grain. On the other hand, as described in Reference 18), it is already known that when the behavior

of grain growth in a 2-D system is considered, whether each individual grain grows or not is determined by the number of sides making up the grain and the argument on the use of the radius, R, mentioned above cannot be supported.

Next, we discuss a matter relating to the number of faces of the grains. The average number of faces that was 14.0 at t = 500 Δt gradually decreased with simulation time to 13.7 at t = 5,000 Δt. These values agree very well with the results obtained by many numerical simulations and with the results of an experimental observation carried out recently.[34] **Fig. 6** shows the distribution of grains with the number of faces per grain. Such geometrical information is extremely difficult to deal with by an mean-field analysis. With microstructural simulation techniques such as the PF method, it is possible to handle even geometrical information directly. For the purpose of comparison, the results obtained by Kim et al. are also shown in Fig. 6. With respect to the number-of-faces distribution too, the result of our simulation agrees well with the result obtained by Kim et al. Then, at t = 6,000 Δt, the linear relation similar to the Aboav–Weaire relations is calculated by the linear least-square fitting for simulation results using the same method as described in Reference 25).[35, 36] As a result, $m\,(Nf) \times Nf = 13.7\,Nf + 24.7$ was obtained. This value is very close to $m\,(Nf) \times Nf = 13.6\,Nf + 27.2$ given by Reference 25), where $m\,(Nf)$ denotes the average number of faces of grains adjoining a grain having Nf faces.

3.2 Simulation of grain growth considering pinning by dispersed particles

This section describes the results of our simulation of grain growth when there are fine dispersed particles of precipitates, nonmetallic inclusions, etc. The "pinning" of crystal growth in a system in which dispersed particles exist is an important means of controlling the crystal grain size. It is also an important phenomenon industrially. More than a half century ago, Zener reported that when inactive, non-coherent, second-phase particles having a radius of r were dispersed in a polycrystalline structure, the average grain size, R, of the parent phase in the ultimate pinned structure in which the grains stopped growing completely was given by the following equation.[37]

$$\langle R \rangle = a \frac{r}{f^b} \tag{6}$$

Where f is the volume fraction of the second-phase particle, and a and b are constants. Under the Smith–Zener assumptions, a = 4/3 and b = 1.[38] Since then, many researchers, including Hillert, have proposed modifications to Equation 6.[39-47]

In addition, experiments have been performed to validate the above equation. Due to the difficulty in 3-D observation of the radius and volume fraction of a small amount of fine particles dispersed in a microstructure, numerical simulations using the MC method,[48-54] or the front tracking method,[55, 56] have been actively carried out since the 1980s. When it comes to discussing the ultimate pinned structure, however, the correct result cannot be obtained unless the system is of considerable size. It requires huge computer resources and much computing time. Besides, with respect to the value of b in the ultimate pinned structure, the results of 2-D and 3-D simulations differ markedly. Concerning 3-D simulations, in particular, they have not yet been completely validated.[38]

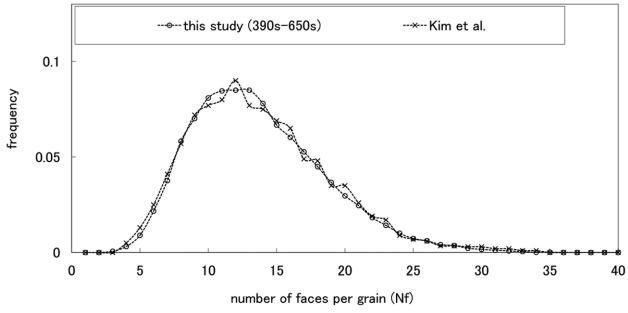

Fig. 6 Distributions of grains with the number of faces per grain in the 3D simulations
Kim et al.[18] (MPF model, symbols were taken from Fig.16 in Ref. 18) and our study (MPF model + APT algorithm)

This section describes the results of our application of the PF method and parallel computation technique to Zener's problem of pinning in a 3-D system.[26] In the simulation, we used the model of Fan et al., a representative MOFM modified by Moelans et al.[55, 56] Concerning the radius of dispersed particles, we found a point of compromise between simulation efficiency and accuracy by assuming r = 2.68 (V = 81 differential lattices).[56] In view of the limited computer resources, the volume fraction, f, of dispersed particles was assumed to be in the range 0.04 to 0.12. For detailed simulation conditions, see Reference 26). In this report, the simulation results obtained when the dispersed particles neither moved nor grew are described. When the PF method is used, however, it is possible to perform a simulation taking into consideration the coarsening of dispersed particles as well.[21]

Fig. 7 shows the time evolution of the microstructure when the f of dispersed particles was assumed to be 0.04. In the figure, the black dots are dispersed particles. **Fig. 8** shows the time evolution in average grain radius of parent-phase grains for various volume fractions, fs, of dispersed particles. At the early stages, the rate of grain growth does not change noticeably since the grain size is small, the number of particles making contact with each grain is small and the interfacial curvature is large. With the growth of grains, the rate of growth decreases and ultimately, the growth stops. **Fig. 9** shows the ultimate pinned microstructures for various volume fractions of dispersed particles.

With the probability of the total number of dispersed particles being present at grain boundaries of the parent phase assumed to be Φ, **Fig. 10** shows the probability of two particles on the interface as Φ_2, the probability of three particles on the edge as Φ_3, and the probability of four particles at the corner as Φ_4. All those probabilities increase with the increase in f. On the other hand, the value of Φ is much smaller than the value obtained by a 2-D simulation despite the fact that the same model parameters were used.[56] The reason for this is that, as pointed out in Reference 56) also, the geometrical arrangement of dispersed particles and interfaces that gives the maximum pinning stress differs between 2-D and 3-D simulations; that is, the interfaces can flee from the dispersed particles more easily in the 3-D simulation.

The value of Φ shown above is also small compared with the result of a 3-D MC simulation by Anderson et al. who treated each dispersed particle as one lattice point and assumed the lattice temperature to be zero.[49] Under their simulation conditions, the growth of grains might have been restrained by artificial facets introduced as a result of the presence of dispersed particles. In order to avoid that problem with the MC method, it is necessary not only to increase the size of dispersed particles sufficiently but also to introduce a heat fluctuation by raising the lattice temperature.[54] In a simulation using the PF method, on the other hand, the interfacial curvature can be expressed accurately and hence, it is possible to obtain a

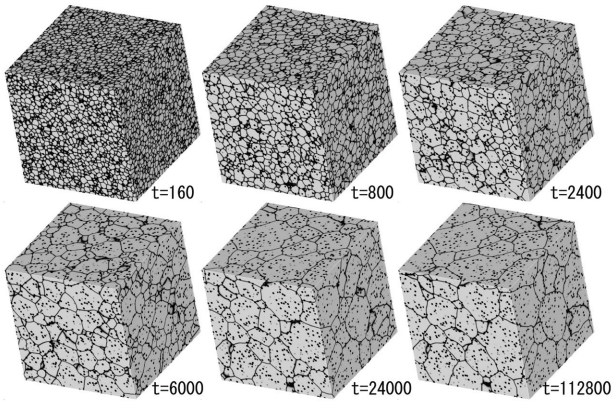

Fig. 7 Simulated microstructural evolution in 400^3 cells for f = 0.04

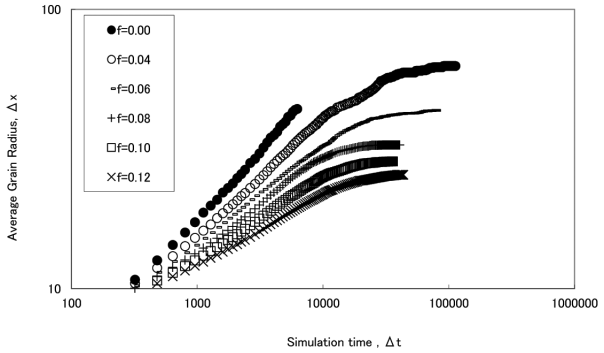

Fig. 8 Average grain radius <R>, versus simulation time for different particle concentrations

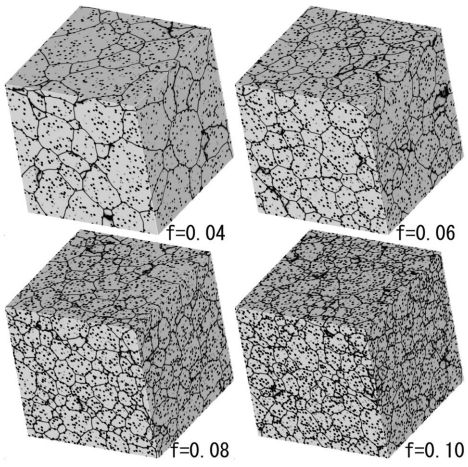

Fig. 9 Pinned microstructures for different particle concentrations f

value of Φ comparable to that shown in Reference 54) without introducing any heat fluctuation.

Fig. 11 shows by means of a log-log graph the relationship between the average grain radius <*R*> of the parent phase in the ultimate pinned microstructure divided by dispersed particle radius *r* and the dispersed particle volume fraction *f*. By applying the least square method to the simulation result and obtaining an approximate

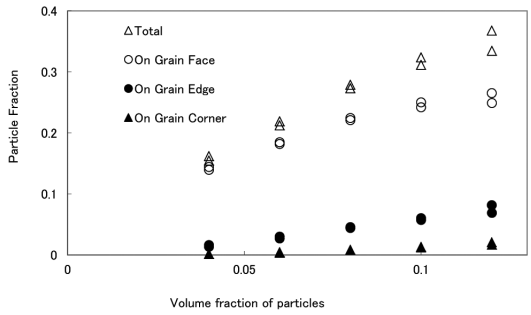

Fig. 10 Fraction of particles on grain faces, edges and corners in the pinned microstructure versus particle concentration f

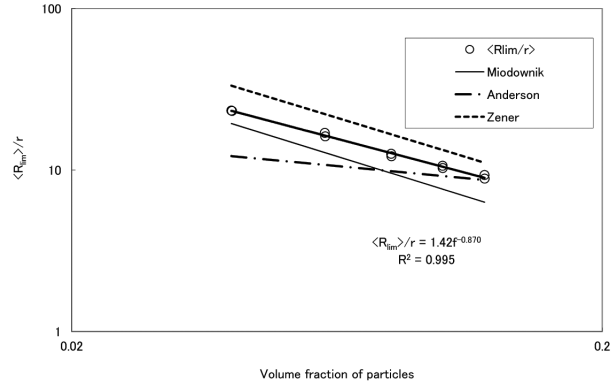

Fig. 11 Average grain radius of the pinned microstructures versus particle concentration f
For comparison, Zener relation[37] and the relations obtained from Monte Calro simulations[49, 54] are plotted.

line, the following relationship was obtained.

$$\langle R \rangle = 1.42 \frac{r}{f^{0.87}} \quad (7)$$

The above relationship is close to the Smith–Zener theory and the result of an MC simulation that assumed a sufficiently large dispersed particle size and introduced a heat fluctuation.[54]

Next, to evaluate the time evoluation of grain size distribution function, the microstructural entropy was defined by the following equation.[57]

$$ME = \frac{\sum_i g_i \ln (g_i)}{\sum_i g_i} \quad (8)$$

Where g_i denotes the proportion of grains which belong to the i^{th} group when the crystal grains are normalized by the average grain size with $g = R/\langle R \rangle$. **Fig. 12** shows the time evolution of microstructural entropy for various values of *f*. When $f = 0$, the microstructural entropy gradually approaches a certain value through the transition region. In a system containing dispersed particles, however, the entropy decreases with simulation time and the size distribution function actually narrows down. The reason for this is that since the average driving force decreases with the progress of grain growth, grains appear which can no longer shrink despite the fact that they are sufficiently smaller than the surrounding grains.

As far as our simulation results are concerned, when $f = 0.04$, there were no grains with a radius of 0.3 <*R*> or less in the ultimate

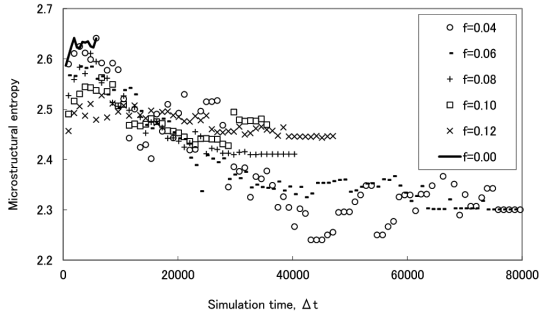

Fig. 12 Temporal evolution of the microstructural entropy ME, for different particle concentrations

pinned microstructure. The above phenomenon in which the size distribution function narrows down in grain growth taking dispersed particles into consideration has also been observed in numerical simulations using mean field approximation.[58, 59] On the other hand, in the case of 2-D simulations, as reported in Reference 56), the size distribution function widens or narrows according to the initial arrangement of dispersed particles and the value of *f*.

4. Conclusion

We have so far described the results of our grain growth simulation by applying the PF method to the normal growth of grains in a single-phase material and the pinning phenomenon of a system containing fine dispersed particles, with the focus on the differences between 2-D and 3-D simulations. With the progress of 3-D structural analysis techniques in recent years, attempts are being made to experimentally clarify 3-D geometric characteristics of polycrystalline microstructures.[34] The application of such experimental analyses in combination with mathematical techniques and numerical simulations will help clarify the mechanisms of structural formation of polycrystalline materials. For example, we consider that it will contribute in the development of a process for manufacturing polycrystalline structures with the desired grain size distribution and grain orientation distribution. In many cases, evaluating the material properties of a polycrystalline structure requires the polycrystalline structure itself as an input value. In this respect, the structure obtained by a simulation using the PF method can be used as that input value.

References

1) Atkinson, H. V.: Acta Metall. 36, 469 (1988)
2) Weaire, D. et al.: Materials Science Forum. 94-96, 27 (1992)
3) Hillert, M.: Acta Metall. 13, 227 (1965)
4) Burke, J. E. et al.: Prog. Metal phys. 3, 220 (1952)
5) Louat, N. P.: Acta Metall. 22, 721 (1974)
6) Weaire, D. et al.: Phys. Rev. Lett. 65, 3449 (1990)
7) Weaire, D. et al.: Phil. Mag. B48, 245 (1983)
8) Weaire, D. et al.: Phil. Mag. Lett. 62, 427 (1990)
9) Kawasaki, K. et al.: Phil. Mag. B60, 399 (1989)
10) Thompson, C. V. et al.: Acta Metall. 35, 887 (1987)
11) Wakai, F. et al.: Acta Mater. 48, 1297 (2000)
12) Anderson, M. P. et al.: Acta Metall. 32, 783 (1984)
13) Srolovitz, D. J. et al.: Acta Metall. 32, 793 (1984)
14) Fan, D. et al.: Acta Mater. 45, 611 (1997)
15) Fan, D. et al.: Acta Mater. 45, 1115 (1997)
16) Kazaryan, A. et al.: Acta Mater. 50, 2491 (2002)
17) Ma, N. et al.: Acta Mater. 50, 3869 (2002)
18) Kim, S. G. et al.: Phys. Rev. E74, 061605 (2006)
19) Warren, J. A. et al.: Acta Mater. 51, 6035 (2003)
20) Kim, S. G. et al.: Acta Mater. 56, 3739 (2008)
21) Fan, D. et al.: Acta Mater. 45, 3297 (1997)
22) Krill, C. E. et al.: Acta Mater. 50, 3059 (2002)
23) Vedantam, S. et al.: Phys. Rev. E73, 016703 (2006)
24) Gruber, J. et al.: Model. Simul. Mater. Sci. Eng. 14, 1189 (2006)
25) Suwa, Y. et al.: Comput. Mater. Sci. 40, 40 (2007)
26) Suwa, Y. et al.: Scripta Mater. 55, 407 (2006)
27) Suwa, Y. et al.: Mat. Trans. 49, 704 (2008)
28) Koyama, T.: Materia Japan. 42, 379 (2003)
29) Koyama, T.: Ferrum. 9, (240, 301, 376, 497, 905), (2004)
30) Allen, S. M. et al.: Acta Metall. 27, 1085 (1979)
31) Steinbach, I. et al.: Physica. D134, 385 (1999)
32) Suwa, Y. et al.: CAMP-ISIJ. 23, 348 (2010)
33) Kim, S. G. et al.: J. Crystal Growth. 261, 135 (2004)
34) Rowenhorst, D. J. et al.: Acta Mater. 58, 5511 (2010)
35) Aboav, D. A.: Metallography. 5, 251 (1970)
36) Weaire, D. et al.: Contemporary Physics. 25, 59 (1984)
37) Smith, C. S.: Trans. AIME. 175, 15 (1948)
38) Manohar, P. A. et al.: ISIJ Int. 38, 913 (1998)
39) Ryum, N. et al.: Scrita Metall. 17, 1281 (1983)
40) Nes, E. et al.: Acta Metall. 33, 11 (1985)
41) Ringer, S. P. et al.: Acta Metall. 37, 831 (1989)
42) Gladman, T.: Proc. R. Soc. Lond. Ser. A294, 298 (1966)
43) Haroun, N. A. et al.: J. Mater. Sci. 3, 326 (1968)
44) Hellman, P. et al.: Scand. J. Metall. 4, 211 (1975)
45) Louat, N.: Phil. Mag. A47, 903 (1983)
46) Hillert, M.: Acta Metall. 36, 3177 (1988)
47) Hunderi, O. et al.: Acta Metall. Mater. 40, 542 (1992)
48) Srolovitz, D. J. et al.: Acta Metall. 32, 1429 (1984)
49) Anderson, M. P. et al.: Scripta Metall. 23, 753 (1989)
50) Hassold, G. N. et al.: Scripta Metall. 24,101 (1990)
51) Kad, B. K. et al.: Mater. Sci. Eng. A238, 70 (1997)
52) Gao, J. et al.: Acta Mater. 45, 3653 (1997)
53) Soucail, M. et al.: Mater. Sci. Eng. A271, 1 (1999)
54) Miodownik, M. et al.: Scripta Mater. 42, 1173 (2000)
55) Moelans, N. et al.: Acta Mater. 53, 1771 (2005)
56) Moelans, N. et al.: Acta Mater. 54, 1175 (2006)
57) Sugden, A. A. B. et al.: Recent Trends in Welding Science and Technology. Ohio, 1989, ASM International
58) Hunderi, O. et al.: Acta Metall. 30, 739 (1982)
59) Abbruzzese, G.: Acta Metall. 33, 1329 (1985)

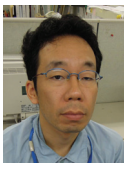

Yoshihiro SUWA
Senior Researcher, Dr.Eng.
Sheet Products Lab.
Steel Research Laboratories
20-1, Shintomi, Futtsu, Chiba 293-8511